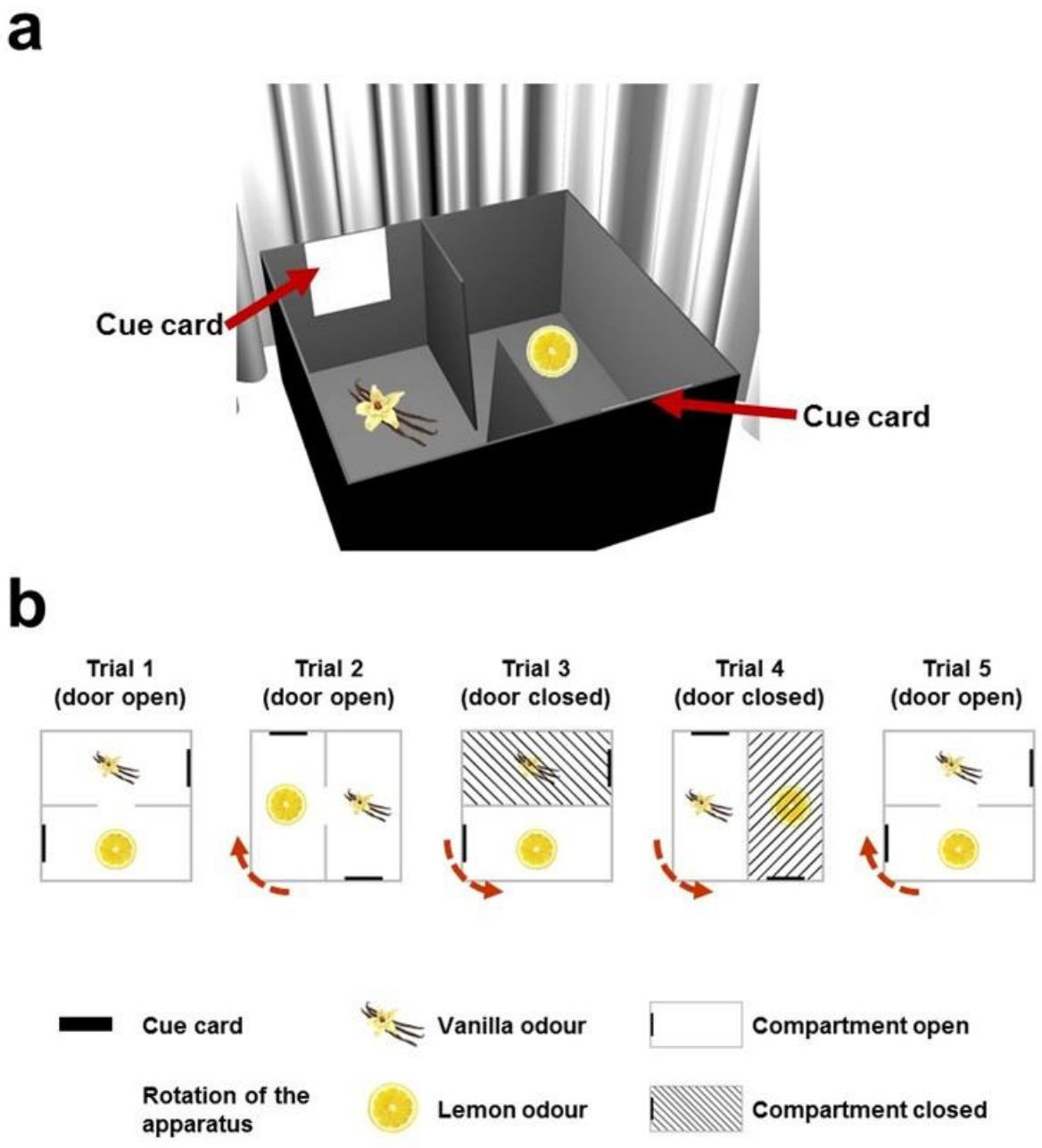

Supplementary Data Figure 1: Experimental setup and recording protocol. a, Schematic of the two-compartment apparatus, with one compartment scented with lemon and one with vanilla. Note that the global two-compartment reference frame has 180-degree rotational symmetry so without the odours, a rat randomly placed in one or other compartment would not know which way it was facing. With the odours, symmetry is broken, so consistent firing of a HD cell across repeated trials indicates use of odour to inform the directional signal. **b**, Protocol for recording trials. The entire apparatus was rotated within the curtained-off arena between trials so as to remove the influence of uncontrolled distal cues. In trials 3 and 4, the rat was randomly placed in one or other compartment, and the door closed to confine the rat to that compartment.

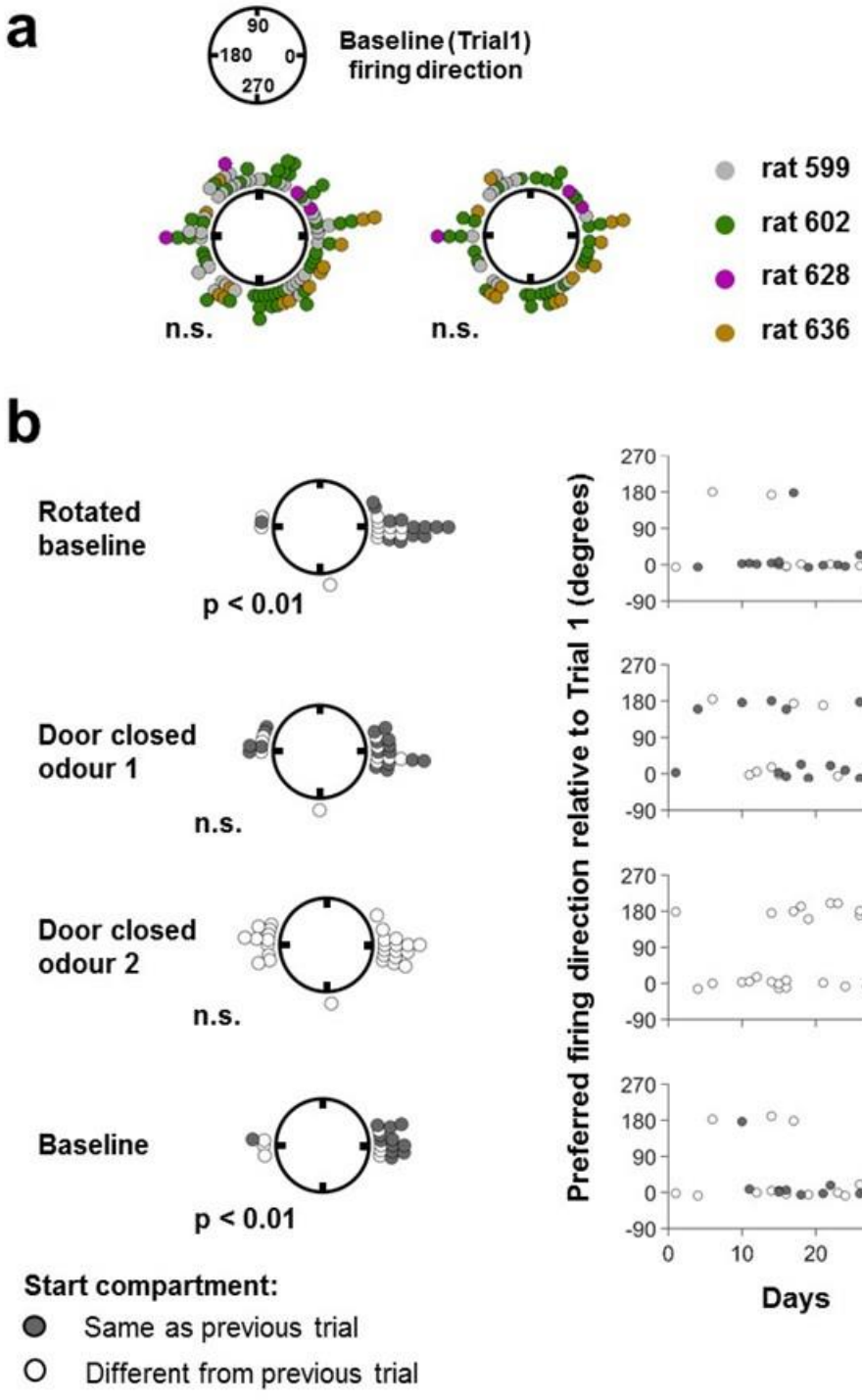

Supplementary Data Figure 2: Directional firing of RSC head direction cells. a, Firing directions in baseline Trial 1 for all RSC HD neurons (left; n = 96) or for the subset recorded in random-start conditions (right; n = 59). Data reveal a homogeneous distribution (n.s. Rayleigh test). **b**, Data for trials 2-5 for the 28 random-start ensembles (averaged across cells in an ensemble), this time oriented relative to the firing direction in baseline trial 1 (set to zero degrees: directions shown by the compass rose). Left: polar plots showing the data collapsed across time; p-values indicate deviation from bimodality. Right: the same data linearized and plotted as a function of recording day. There was significant preference for the original firing direction in some trials, but also significant ambiguity (see Supplementary results for details). Therefore, the HD system can use odour cues to break environmental symmetry, but this effect is weak.

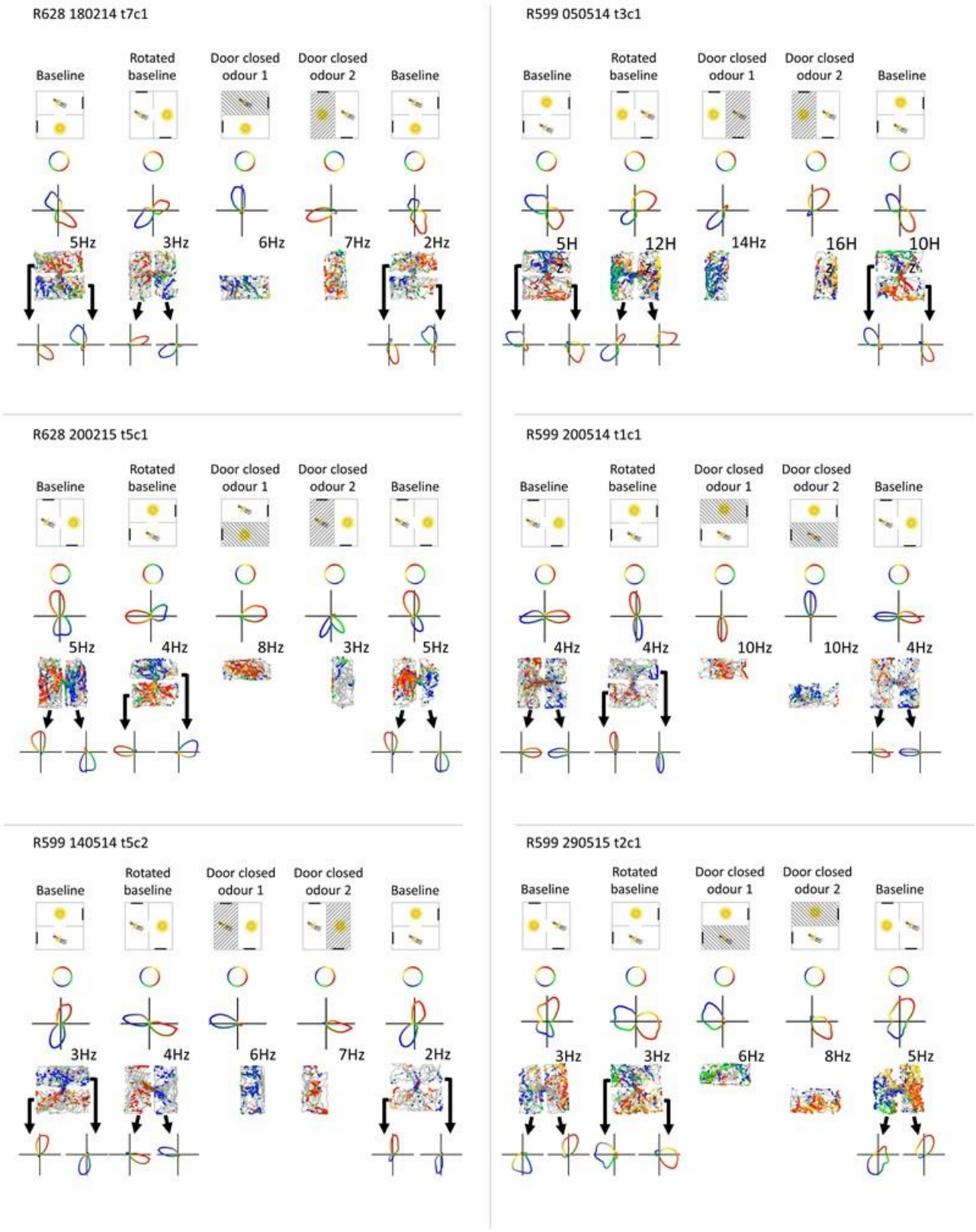

Supplementary Data Figure 3: Polar plots from six bipolar head direction cells showing bimodal firing, with two tuning curves at 180 degrees, illustrated as in Fig. 1. Note that when firing is analysed for only one compartment the tuning curves become unimodal, indicating directional firing that is compartment-specific and reverses between the compartments. The directionally color-coded spatial spike plots (fourth row of each panel) confirm the compartment-specific distribution of directionality.

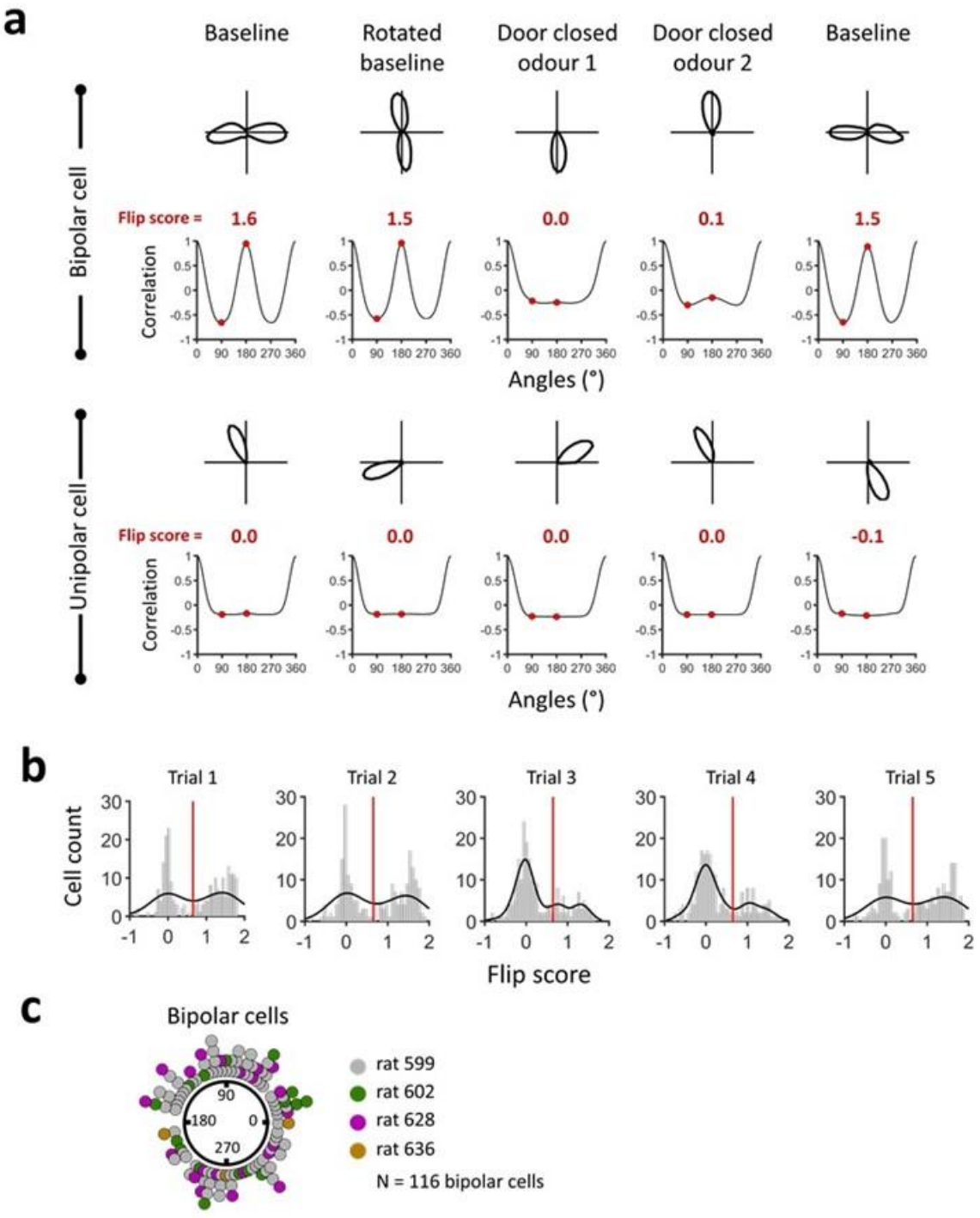

Supplementary Data Figure 4: Calculation of the bimodality of directional firing (the 'flip score'). a, Computation of the flip score for a bipolar (top) and an unipolar (bottom) HD cell across five recording trials. The flip score is the difference of correlation values at 180° and 90° extracted from the circular autocorrelogram. **b**, Distribution of flip score values of bipolar and unipolar HD cells, showing the bimodality and the index. The black line shows the kernel density estimation of distributions and the red line is set at the natural splitting of flip score (value equal to 0.6). **c**, Polar distribution of firing direction of all 116 RSC bipolar HD cells after using the double angle procedure. Each dot corresponds to a bipolar cell firing direction and is color-coded according to rat (n = 4). There was no significant clustering of firing direction (Rayleigh test).

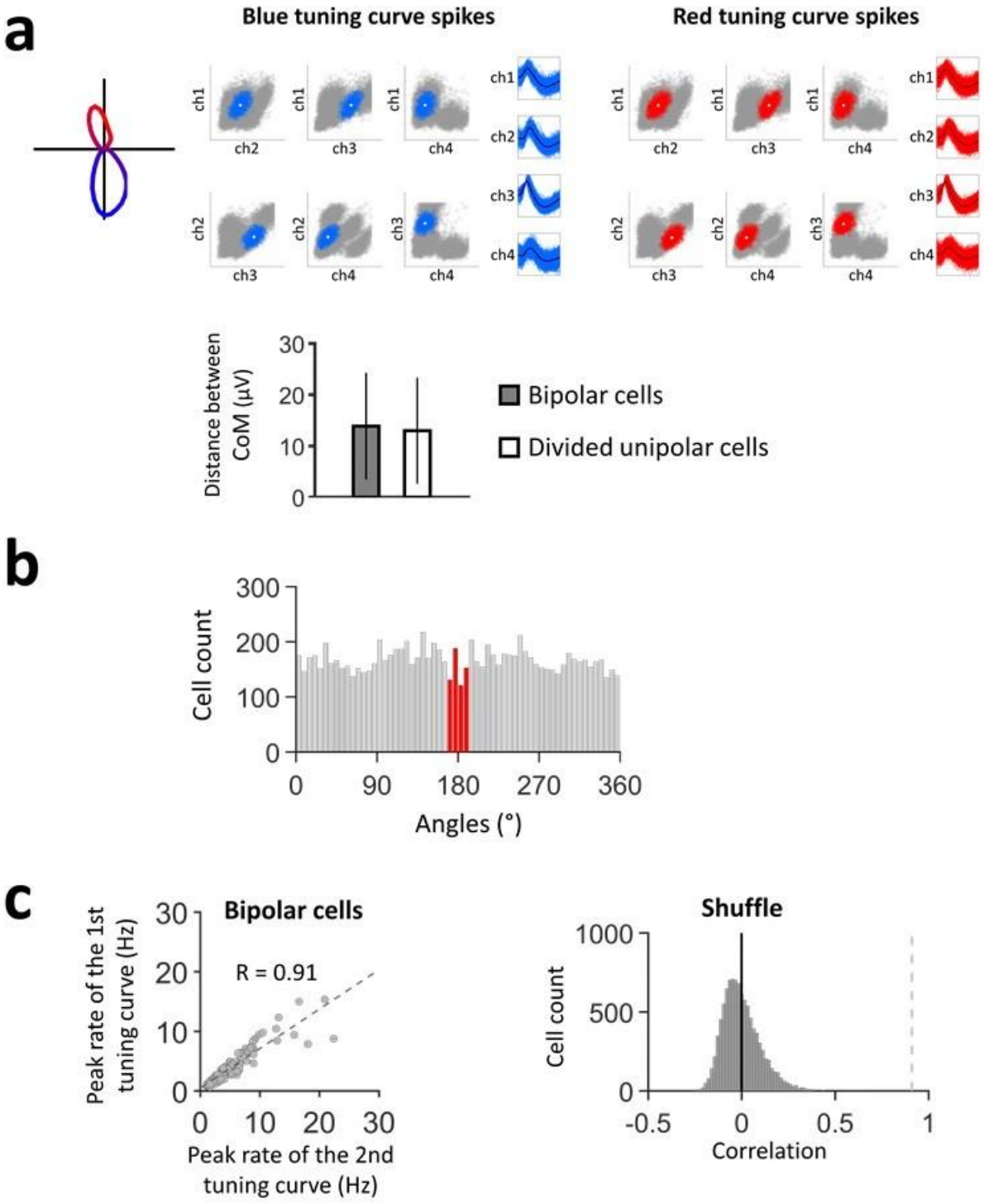

Supplementary Data Figure 5: Ruling out that bipolar tuning curves might have been two cells poorly separated. a, Cluster space analysis: the centres of mass (CoM) of clusters from the individual bipolar cell tuning curves were no further apart in cluster space than for unipolar cells randomly divided in two. **b**, The angles between randomly selected pairs on unipolar cells yielded tuning curves near 180 degrees apart only 4% of the time (red bars) whereas 100% of the double-tuning curve cells in our data had angular separations that fell within this range. **c**, Firing rates between the individual tuning curves of bipolar cells were highly correlated (left) whereas the distribution for randomly selected pairs of unimodal cells was around zero (right), the data falling far outside this range (dotted line).

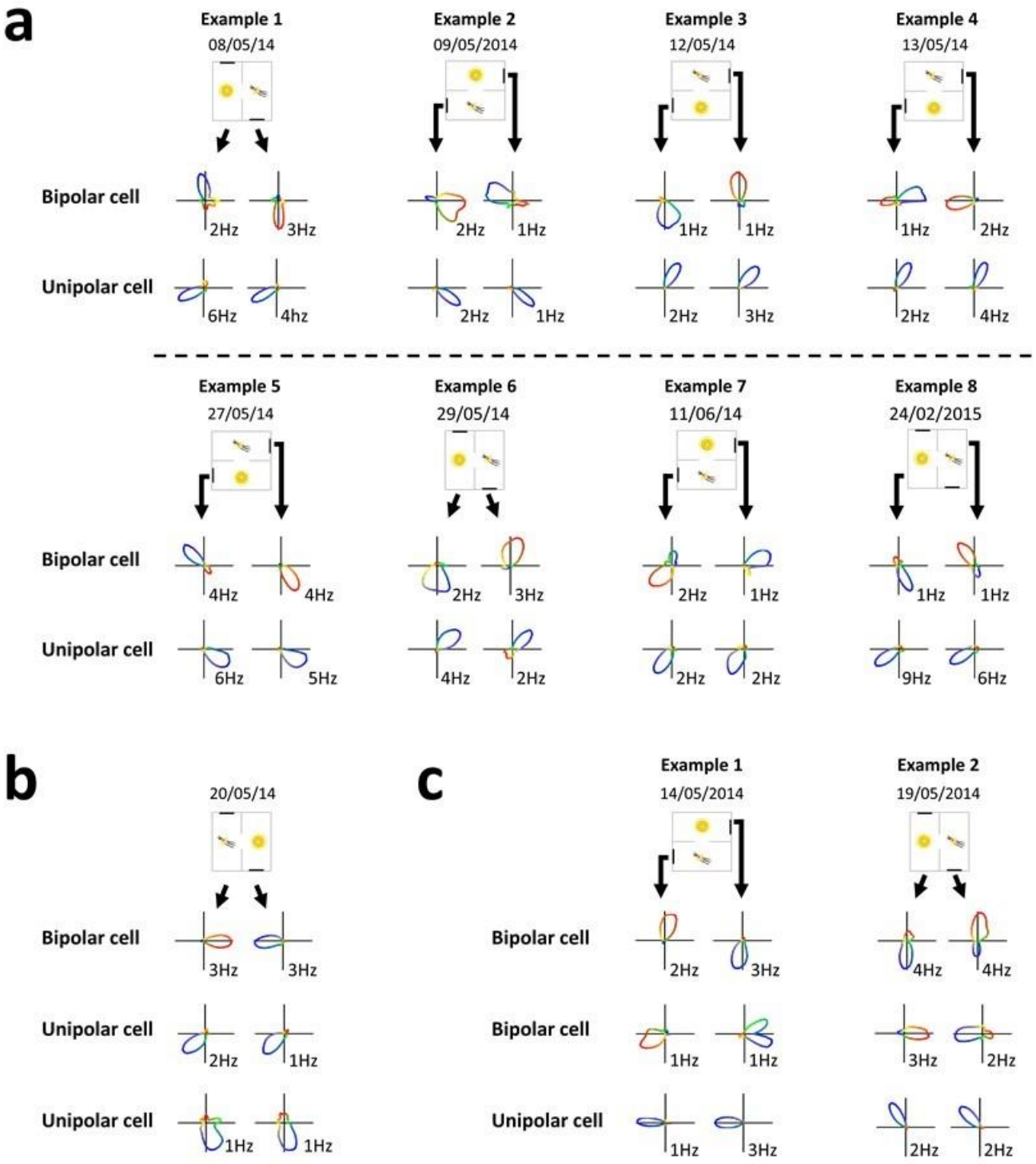

Supplementary Data Figure 6: Co-recording of bipolar and HD cells reveals dissociation between tuning curve directions in different compartments. a, Eight examples, from six different days and three different animals, of simultaneous recordings of bipolar and unipolar HD cells. **b**, Example of one bipolar HD cell simultaneously recorded with two unipolar HD cells. **c**, Two examples of two bipolar HD cells with two different firing directions simultaneously recorded with one unipolar HD cell. In all these examples, note that the bipolar HD cell tuning curves reverse between compartments while the HD tuning curves do not.

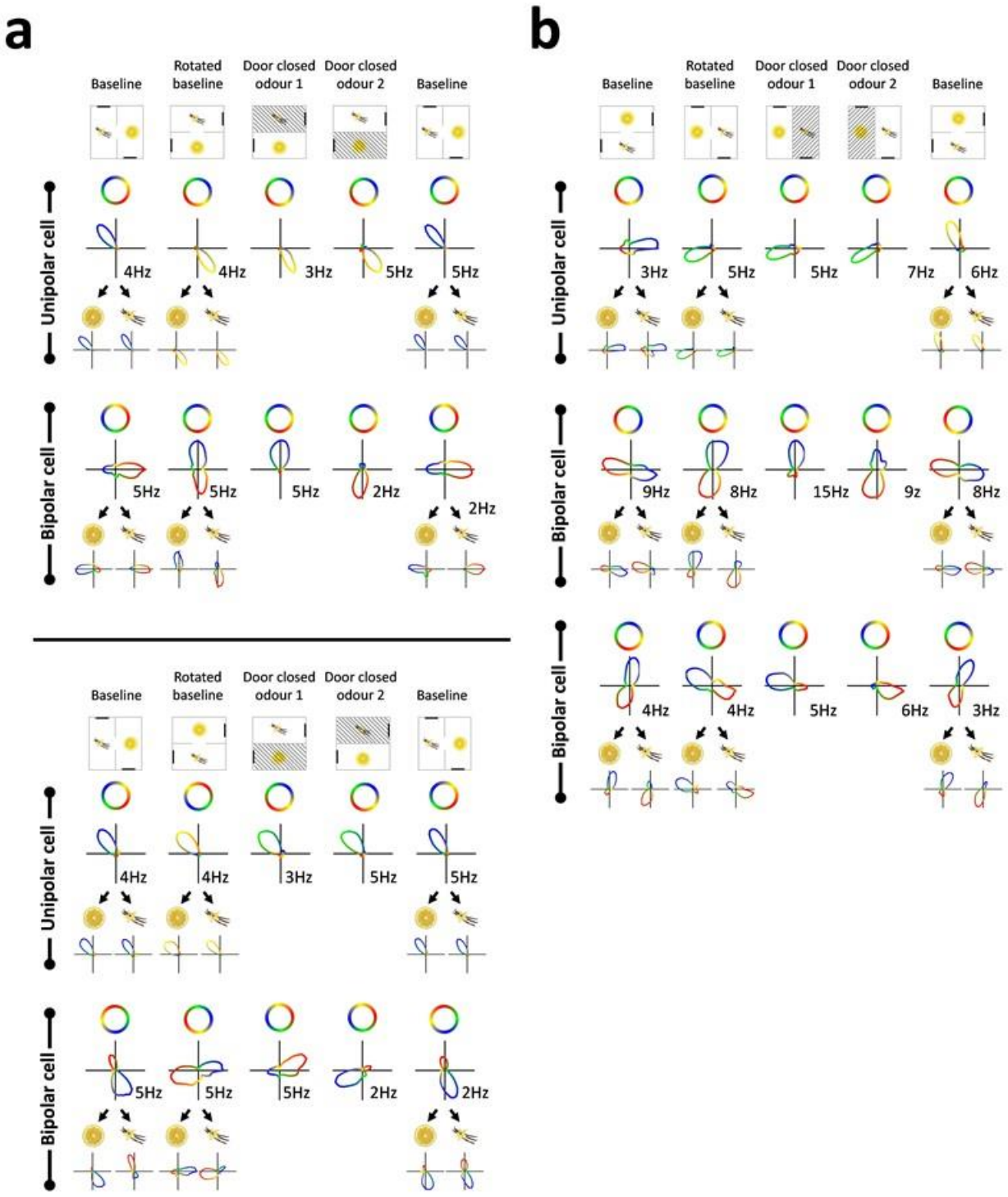

Supplementary Data Figure 7: Disjunctive rotations of unipolar and bipolar HD cells further reveal dissociated directionality. a, Simultaneous recordings of unipolar and bipolar HD cells from two recording sessions (top and bottom). **b**, Example of an unipolar HD cell simultaneously recorded with two bipolar HD cells. Unipolar HD cells show incoherent rotations of their firing directions relative to apparatus rotations, while bipolar HD cells follow these apparatus rotations. This demonstrates uncoupling within the unipolar attractor network, and suggests stronger control by visual cues over bipolar HD cells than unipolar HD cells.

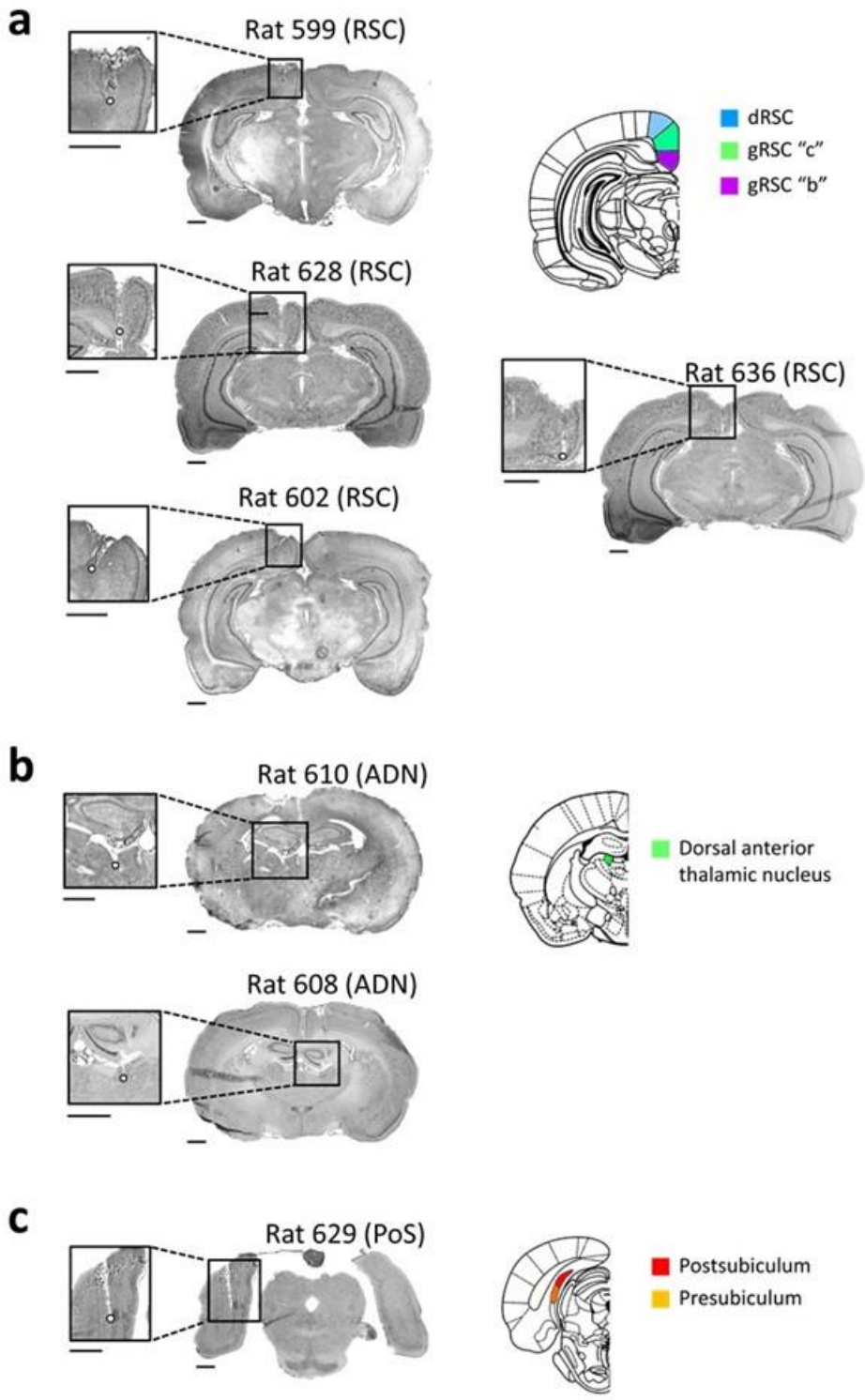

Supplementary Data Figure 8: Histology. Coronal slices through the region of electrode implantation from (**a**) the retrosplenial animals (RSC), (**b**) the anterodorsal nucleus of the thalamus (ADN), and (**c**) postsubiculum (PoS). Main images are at low power and insets at high, with scale bars indicating 1 mm. The hollow dots show the deepest location at which directional neurons were found, estimated using the line drawings (right) adapted from Paxinos and Watson (2007).

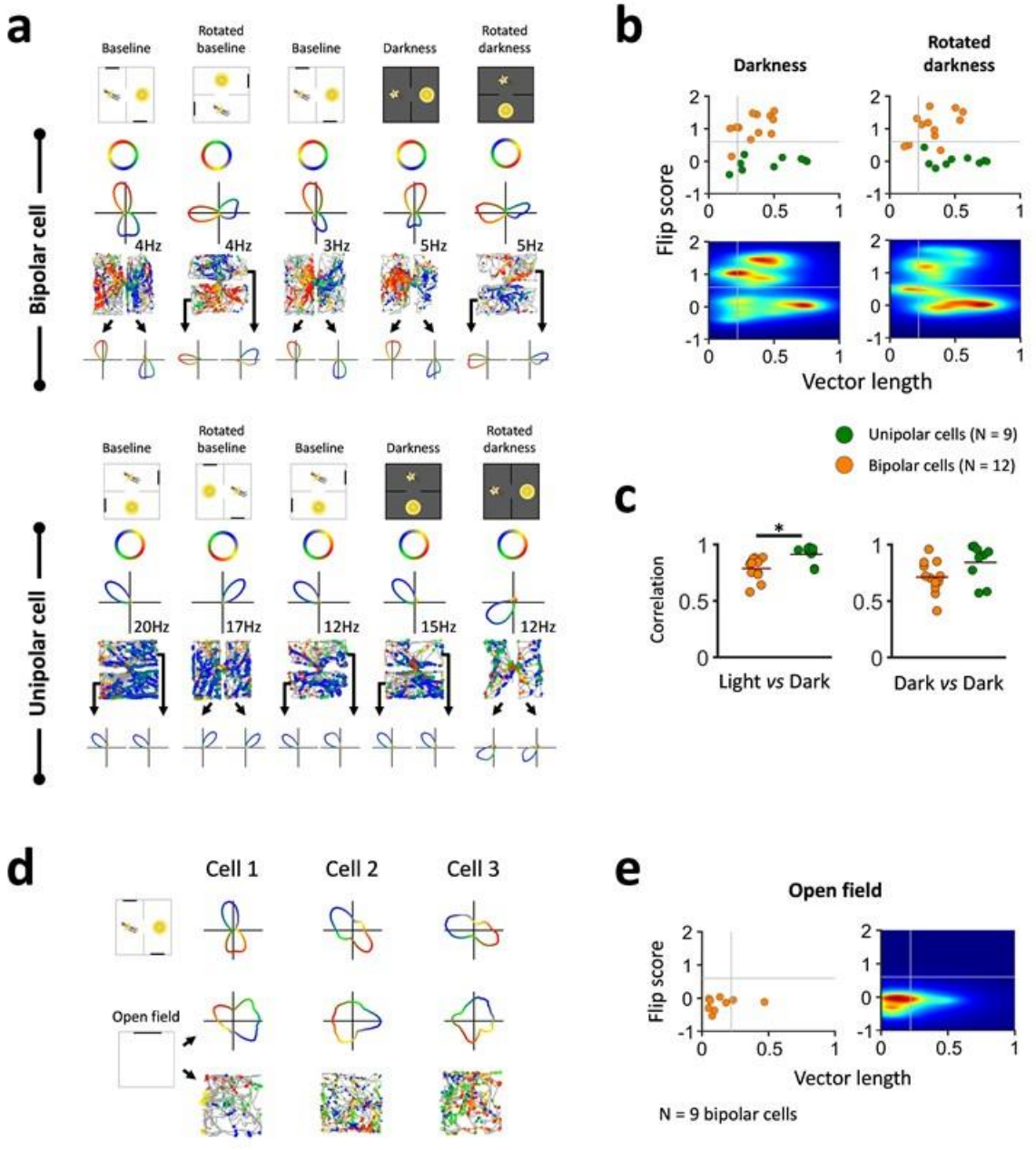

Supplementary Data Figure 9: Preservation of firing direction reversal in the dark, but not in an open field. a, Examples of bipolar and unipolar HD cells recorded during two darkness trials, showing preserved directionality. **b**, Scatter and data density distribution of the population of RSC bipolar cells and unipolar HD cells recorded in darkness, showing a similar distribution between the two populations in darkness as in light. **c**, Correlation of bipolar and HD cells between light-dark trials (baseline – darkness) and dark-dark trials (darkness – rotated darkness), showing maintained high correlation in darkness. **d**, Examples of three bipolar cells recorded in an open field. No clear directional activity is apparent. **e**, Scatter and data density distribution showing that 9 bipolar cells lost both directional and bipolar pattern in an open arena.

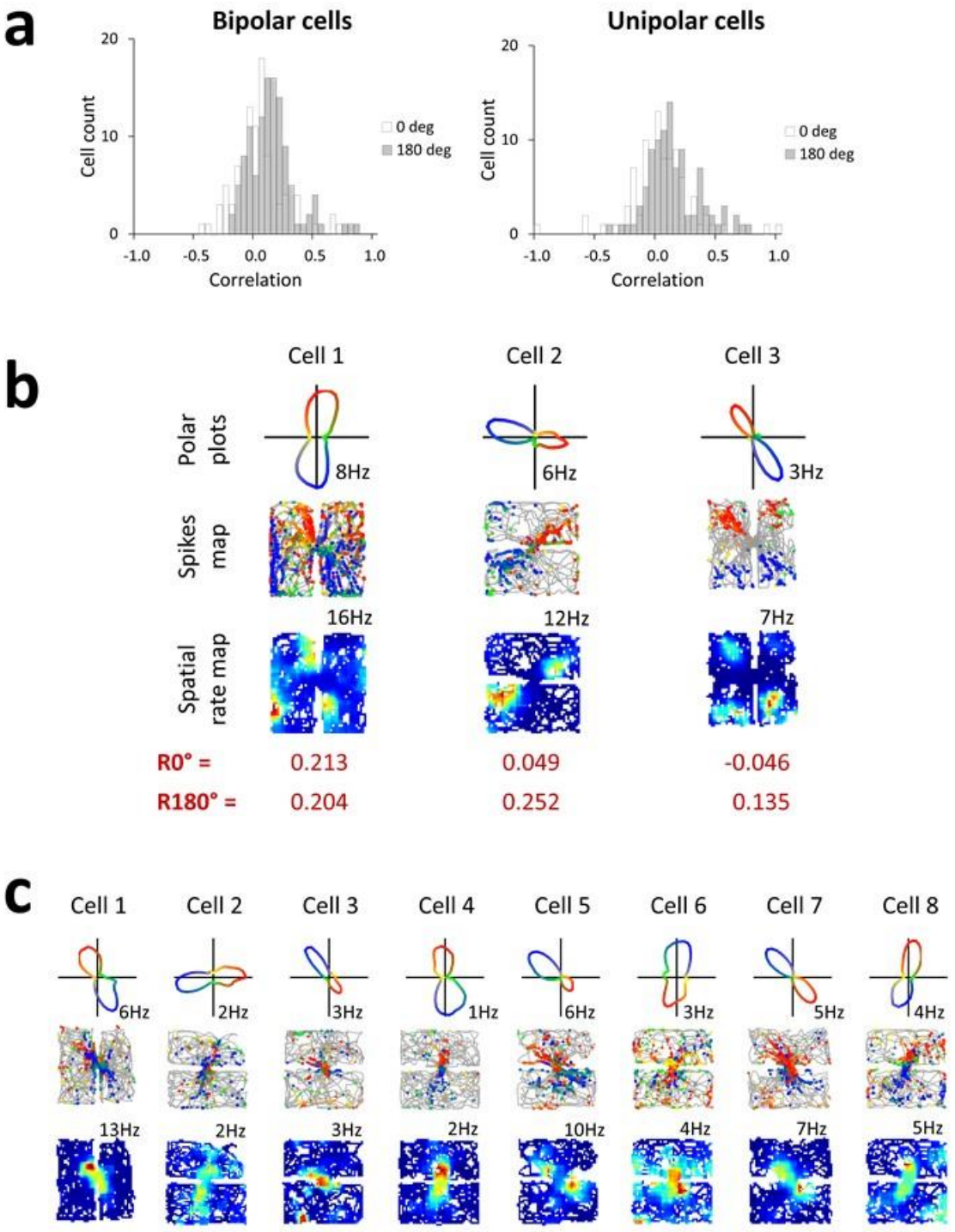

Supplementary Data Figure 10: Spatial patterns of firing. a, Examples of four bipolar cells showing a spatial pattern. Correlation values are reported for spatial correlation computed between the two compartments in their original configuration (0°) or with one compartment rotated by 180°. **b**, Eight bipolar cells showing spatial activity related to the doorway. **c**, Distributions of spatial correlations computed between spatial rate maps of lemon and vanilla compartments for bipolar (left) and HD (right) cells for trial 1. Light grey: distributions of spatial correlations between the two compartments at 0° (R0°), dark-grey: distributions of spatial correlations between the vanilla spatial map rotated at 180° and the lemon spatial map non rotated (R180°).

Supplementary information

Ruling out cell isolation or tracking artefacts

Having identified that a subpopulation of RSC neurons expressed two opposing tuning curves (Figs. 1 and Supplementary Data Fig. 3), we ran several analyses to rule out that these could have been due to isolation or tracking artefacts.

These were unlikely to have been pairs of unimodal cells for the following reasons. First, we found that the spike clusters from each bipolar cell tuning curve were just as closely overlying in cluster space as those of single classic HD cells randomly subdivided into two (Supplementary Data Fig. 5a). The Euclidean distance in μV between the centres of mass (CoM) of these clusters was compared with the distance generated by a control procedure, in which 96 HD cell clusters were arbitrarily divided in two 400 times, and the distances of the resulting sub-clusters calculated and then averaged. Mean CoM distance between the two sub-clusters of bipolar cells was 15μV ±11.79; mean CoM distance for the randomized data was 16.57μV ±12.74; these did not differ [$t(38514)= -1.428$, n.s.]. Second, the individual tuning curves of bipolar cells were always near 180 degrees, which was highly unlikely by chance (Supplementary Data Fig. 5b). This was determined using a random selection of cell-pairs which yielded tuning curves that differed by 180 +/- 12 degrees (red bars) only 4% of the time, compared to the bimodal cells in the data set in which all 169 cells fell within this range of tuning curve separation. ($\chi2(1) = 185$, $p < 0.0001$). Third, peak firing rates for the individual tuning curves of the bipolar cells were highly correlated ($R = 0.91$; Supplementary Data Fig. 5c left) whereas for randomly selected cell-pairs the firing rates showed a low correlation ($R = 0.00 \pm 0.01$; Supplementary Data Fig. 5c right), which the value for the data (dotted line) far exceeded ($z = 12.04$, $p < 0.00001$). Fourth, many bipolar cells showed compartment-specific activity, meaning that the individuals in the putative cell-pairs would have to have fired in only one compartment, which has never been observed in HD cells.

We can also rule out confusion of the large vs small headstage lights (used to determine head direction). *A priori* it seems unlikely that crossing a doorway should reverse apparent light size, and the observing experimenter saw no evidence of this. It is also not clear why such an artefact should affect only recordings from one of the sampled brain regions. However, that bipolar and unipolar cells were co-recorded (e.g. Fig. 1d) is the definitive proof that the bipolarity was not due to light-swapping (because it would have affected all cells together).

Odour-context encoding

We investigated whether RSC HD cells can use the odour information to orient their activity when the rats are randomly placed in one or other compartment (Supplementary Data Fig. 2). We referred all firing directions to the direction established in the lemon compartment in Trial 1, and expressed firing directions in the remaining trials as a deviation from this. Because HD cells tend to rotate coherently, values for co-recorded cells were averaged to provide an ensemble value. Ensembles and trials were, however, treated as independent data points.

28 ensembles were recorded over 4 trials, totalling 112 data points. We compared the data against the null hypothesis of no use of olfactory cues and thus inability to distinguish the two apparatus orientations (predicting an even distribution between the zero +/- 30 degree sector and the 180 +/- 30 degree sector), and an alternative hypothesis of perfect use of olfactory cues (predicting a clustering of firing directions around zero +/- 30 degrees). The predictions and data are shown in Table S1 below, which shows that the behaviour of the cells revealed an above-chance, but incomplete, use of olfactory cues to disambiguate the compartments.

	Hypotheses		
Predicted clustering of data points	**No use of olfaction**	**Use of olfaction**	**Data**
-30 to +30 degrees	54	108	82
150 to 210 degrees	54	0	26
Total	**108**	**108**	**108**
Chi-square value testing hypothesis against data	15.56	29.56	
P value	< 0.0001	< 0.0001	

Table S1: Analysis of olfactory disambiguation of compartments. Data are collapsed across trials: the p-values for analyses of individual trials are shown in Supplementary Data Fig. 2.

Firing in the dark

We removed visual cues by turning off the lights, to see if directional firing would degrade. We recorded RSC and PoS cells first in light and then in two dark trials (n = 12 sessions), the first being a continuation of the last trial, then a second dark trial after removal, mild disorientation and a rotation of the environment. Despite a slight (although significant) decrease of the directional stability in darkness (Kruskal-Wallis, $p < 0.05$), cross-correlation of bipolar and HD cells (n = 14 cells) remained high between the two dark trials (light/light = 0.84; light/dark = 0.81; dark/dark = 0.73), indicating that the bipolar firing is maintained without visual information (Supplementary Data Fig. 9 a, b, c). Consistent with previous observations (Chen, Lin, Green, *et al.*, 1994), 'classic' HD cells from RSC (n = 9) also maintained their directional firing in darkness. In addition, high correlation values indicate that both type of HD cells rotated coherently with the apparatus during the second dark trial,

suggesting that the door and odour information provided local and contextual information helping to maintain directional activity.

LFP/spiking characteristics and movement correlates

Firing rates and inter-spike intervals

Peak firing rates were as follows: RSC bipolar = 5.10 +/- 0.37 Hz, RSC unipolar = 7.54 +/- 0.87 Hz, PoS = 5.13 +/- 0.55 Hz and ADN = 18.17 +/- 2.60 Hz. One-way ANOVA found a significant effect [$F(3,278) = 26.3$, $p < 0.0001$]; post hoc tests (Bonferroni corrected) showed that ADN rates were significantly higher than RSC bipolar cells [$t(145) = 8.62$, $p < 0.001$], RSC unipolar cells [$t(125) = 5.0$, $p < 0.001$] and PoS HD cells [$t(68) = 5.44$, $p < 0.001$].

The inter-spike interval histogram showed peak latencies as follows: RSC bipolar = 35.24 +/- 2.86 ms, RSC unipolar = 38.35 +/- 4.11 ms, PoS = 35.05 +/- 12.82 ms and ADN = 18.16 +/-4.21 ms. The values were highly skewed so the ANOVA was conducted on the log-transformed data and showed a significant effect [$F(3,120) = 4.2$, $p < 0.01$]; post hoc tests (Bonferroni-corrected) showed that the ADN time-to-peak was significantly shorter than RSC bipolar cells [$t(124) = 3.03$, $p = 0.02$] and unipolar cells [$t(145) = 3.85$, $p = 0.001$] but not PoS HD cells [$t(68) = 1.91$, NS]. The other cell types did not differ. The decay time to half-peak, which is a measure of the proportion of longer intervals in the spike train, was also shorter for ADN neurons. ANOVA showed that this was significant [$F(3,277) = 9.60$, $p = 0.0001$]; post hoc tests (Bonferroni-corrected) showed that it was shorter than RSC bipolar cells [$t(145) = 4.90$, $p < 0.01$] and unipolar cells [$t(124) = 4.27$, $p = 0.001$] but not shorter than PoS HD cells [$t(68) = 2.16$, NS]. The other cell types did not differ. Taken together, these data show that ADN neurons fired at a higher rate but there was no difference between the other cell types; in particular, bipolar HD cells in RSC were not discernibly different in their basic firing characteristics.

LFP theta and speed-theta correlation

Theta band LFP activity is thought to be important in spatial coding so we looked at this at both the population and single cell level. The LFP showed a peak in the theta band for recordings from all three brain areas (RSC peak = 8.89 +/- 0.03Hz, PoS = 9.01 +/- 0.07, ADN = 8.56 +/- 0.28). Theta power, expressed as the ratio of theta to delta, was higher in RSC (RSC = 3.24 +/- 0.27, PoS = 1.97 +/- 0.73, ADN = 0.91 +/- 0.05). ANOVA revealed a significant effect [$F(2,100) = 8.20$, $p = 0.0005$]) and post-hoc testing (Bonferroni corrected) showed that theta power in RSC was non-significantly higher than in PoS ($t(85) = 1.75$, $p = 0.24$) but significantly higher than in ADN [$t(88) = 3.94$, $p = 0.0006$].

Individual cells showed spiking at theta frequency, which did not differ between brain areas, nor between bipolar and unipolar HD cells in RSC (RSC: bipolar = 8.78 +/1 0.12 Hz, unipolar = 8.55 +/- 0.13Hz, PoS = 8.93 +/- 0.02, ADN = 8.93 +/- 0.19; [$F(3,274) = 1.3$, NS]). However, theta power in the spiking histograms was very low, with a theta/delta ratio of close to zero for all cell types except, interesting, the bipolar RSC cells, in which it was 0.44. ANOVA revealed a significant difference [$F(3,274) = 16.5$, $p = 0.0001$] and post-hoc testing (Bonferroni corrected) showed that theta power RSC bipolar cells was higher than in unipolar cells [$t(206) = 5.32$, $p < 0.001$] and PoS HD cells [$t(153) = 3.46$, $p < 0.01$], and higher but not-quite-significantly than ADN HD cells [$t(145) = 3.08$, $p = 0.06$]. There was no correlation with running speed (not shown). Since angular movements are important for head direction neurons, we also looked at the relationship between cell firing rate and angular head velocity (AHV) but also saw no relationship.

Spatial correlates of firing

Previous studies have reported spatial activity in RSC neurons (Cho & Sharp, 2001) and so we looked for spatial correlates of firing in the directional neurons. We found a small number of bipolar HD cells showing spatial-by-bipolar conjunctive activity (Supplementary

Data Fig. 10). However, spatial correlations between each compartment reveal that the spatial pattern is not a major component of bipolar cells. It is interesting to note that most of the spatially localized activity is located at the doorway between the compartments, although some spatial patterns were also seen elsewhere in the apparatus (Supplementary Data Fig. 10 b, c).